View metadata, citation and similar papers at core.ac.uk
brought to you by CORE
provided by Open Access Repository

BARI-TH/326-98, hep-ex/9901012

Test of non-standard neutrino properties with the BOREXINO source experiments

A. Ianni[a,b] *, D. Montanino[c] †, and G. Scioscia[d] ‡
[a] *Dipartimento di Fisica dell'Università dell'Aquila, Località Coppito, I-67010 L'Aquila, Italy*
[b] *Laboratori Nazionali del Gran Sasso, S.S. 17bis Km 18+910, I-67010 Assergi (L'Aquila)*
[c] *Scuola Internazionale Superiore di Studi Avanzati (S.I.S.S.A.), Via Beirut 4, I-34014 Trieste, Italy*
[d] *Dipartimento di Fisica dell'Università di Bari, Via Amendola 173, I-70126 Bari, Italy*

arXiv:hep-ex/9901012v2 18 Mar 1999

Abstract

We calculate the event rates induced by high-intensity radioactive sources of ν_e (^{51}Cr) and of $\bar{\nu}_e$ (^{90}Sr), to be located near the BOREXINO detector. Calculations are performed both in the standard case and assuming non-standard properties of neutrinos, including flavor oscillations, neutrino electromagnetic interactions, and deviations from the standard vector and axial couplings in the ν_e-e interaction. It is shown that, in some cases, the current limits on non-standard neutrino properties can be significantly improved.

Typeset using REVTEX

*email: ianni@lngs.infn.it

†email: montanin@sissa.it

‡email: scioscia@ba.infn.it

I. INTRODUCTION

The BOREXINO experiment [1–3], under construction at Gran Sasso, is designed to study ^{7}Be solar neutrinos [4] through a real-time, low-background detector, consisting of a nylon sphere (8.5 m in diameter) filled with high purity organic scintillator (pseudocumene, C_9H_{12}).

The apparatus can be calibrated through external (anti-)neutrino sources as well as through light sources [5]. For the first type of calibration experiment, two sources have been considered: ^{51}Cr and ^{90}Sr. The ^{51}Cr source generates ν_e through the reaction $^{51}\mathrm{Cr} + e^- \to {}^{51}\mathrm{V} + \nu_e$, with a half-life $\tau_{1/2}^{\mathrm{Cr}}$ of 27.7 days and four energy lines: $E_1 = 0.751$ MeV (9%), $E_2 = 0.746$ MeV (81%), $E_3 = 0.431$ MeV (1%), $E_4 = 0.426$ MeV (9%).

The ^{90}Sr source generates $\bar{\nu}_e$ through the reaction $^{90}\mathrm{Sr} \to {}^{90}\mathrm{Y} + \bar{\nu}_e + e^-$ ($\tau_{1/2}^{\mathrm{Sr}} \sim 28$ y) followed by $^{90}\mathrm{Y} \to {}^{90}\mathrm{Zr} + \bar{\nu}_e + e^-$ ($\tau_{1/2}^{\mathrm{Y}} \sim 64.8$ h). Since $\tau_{1/2}^{\mathrm{Y}} \ll \tau_{1/2}^{\mathrm{Sr}}$, one can simply assume that two $\bar{\nu}_e$'s are produced for each ^{90}Sr nucleus decay. The total standard spectrum of this source is given by $\lambda(E_\nu) = \lambda_{\mathrm{Sr}}(E_\nu) + \lambda_{\mathrm{Y}}(E_\nu)$, where each λ_i ($i \in \{\mathrm{Sr}, \mathrm{Y}\}$) is calculated using Fermi theory [6]:

$$\lambda_i\left(E_\nu\right) = A_i \frac{x_i}{1 - e^{-x_i}} \left(Q_i + m_e - E_\nu\right) E_\nu^2 \sqrt{\left(Q_i + m_e - E_\nu\right)^2 - m_e^2}\,. \tag{1}$$

In Eq. (1), A_i is a normalization factor [so that $\int dE_\nu \lambda_i(E_\nu) = 1$], Q_i is the endpoint energy ($Q_{\mathrm{Sr}} = 0.546$ MeV and $Q_{\mathrm{Y}} = 2.27$ MeV), m_e is the electron mass, and

$$x_i = 2\pi Z_i \alpha_{\mathrm{e.m.}} \frac{Q_i + m_e - E_\nu}{\sqrt{\left(Q_i + m_e - E_\nu\right)^2 - m_e^2}}\,, \tag{2}$$

Z_i being the atomic number of the decaying nuclei and $\alpha_{\mathrm{e.m.}}$=1/137.036 [7]. The standard ^{90}Sr-^{90}Y spectrum is shown in Fig. 1.

Artificial neutrino sources of known activity and spectra can be used to probe non-standard neutrino properties, such as flavor oscillations or magnetic moment [8–10] or non-standard neutrino couplings (for example through the exchange of an additional Z boson [11]). In particular, in [12] the combined analysis of $\bar{\nu}_e$-e scattering and inverse beta decay using only a ^{90}Sr source has been proposed for studying both oscillation and non-standard neutrino couplings.

In this paper we study in detail how to use the ^{51}Cr and ^{90}Sr sources to probe flavor oscillations, electromagnetic properties, and deviations of the axial and vector couplings $g_V^{\nu e}$ and $g_A^{\nu e}$ from their standard value in ν_e-e scattering. The sensitivity of the experiments depends on the initial activity of the sources, which is constrained by technical and economical budget limits. [1] As a reasonable reference value we use 5 MCi= 1.85×10^{17} decay/s for each source activity.

The plan of this work is the following: in Sec. II we describe the calibration experiments and calculate the standard expectations. In Sec. III we calculate the effect of oscillations into

[1] A high intensity source with a proper shielding costs about 1M$/MCi [13].

active or sterile states and determine the BOREXINO sensitivity to the neutrino mass and mixing. In Sec. IV we study how BOREXINO can probe neutrino magnetic and anapole moments. In Sec. V we show how this experiment can put interesting limits on the ν_e-e vector and axial couplings. Finally, we draw our conclusions in Sec. VI.

II. DESCRIPTION OF THE EXPERIMENT AND STANDARD EXPECTATIONS

In this section we describe the radioactive source experiments and the standard rates induced by the sources. We assume the following technical setup: 100 tons (6×10^{30} protons, 3.3×10^{31} electrons) of spherical ($R = 3$ m) fiducial volume (FV) and 5 MCi pointlike sources placed at distance $D = 8.25$ m from the detector center.

In the ^{51}Cr source experiment (ν_e) the detection process is neutrino-electron elastic scattering, while in the ^{90}Sr experiment ($\bar{\nu}_e$) the interactions are elastic scattering and inverse β-decay. The scattering events are identified through the scintillation light from the electron. The inverse β-decays are identified through the delayed coincidence between the prompt positron annihilation signal and the neutron capture γ's.

The standard (std) differential cross section of the scattering process $\nu_{e,\mu} + e \to \nu_{e,\mu} + e$, as a function of the the incident neutrino energy E_ν and of the recoil electron kinetic energy T_e, is [14]:

$$\frac{d\sigma^{\rm std}_{e,\mu}(E_\nu, T_e)}{dT_e} = \frac{G_F^2 m_e}{2\pi}\left[(C_V + C_A)^2 + (C_V - C_A)^2\left(1 - \frac{T_e}{E_\nu}\right)^2 + \left(C_A^2 - C_V^2\right)\frac{m_e T_e}{E_\nu^2}\right], \quad (3)$$

where $C_{V,A} = g_{V,A}^{\nu e,{\rm std}} + \delta$ and $g_V^{\nu e,{\rm std}} = 2\sin^2\theta_W - \frac{1}{2}$, $g_A^{\nu e,{\rm std}} = -\frac{1}{2}$, with $\delta = 1$ ($\delta = 0$) if the incident neutrino is a ν_e (ν_μ). For antineutrinos, $C_A \to -C_A$. We take $\sin^2\theta_W = 0.2312$ [7].

The cross section in a definite energy window $T_e \in [T_{e,1}, T_{e,2}]$ is given by

$$\sigma_{e,\mu}(E_\nu) = \int_0^{E_\nu/(1+m_e/2E_\nu)} dT_e\, W(T_e)\frac{d\sigma^{\rm std}_{e,\mu}(E_\nu, T_e)}{dT_e}, \quad (4)$$

where $W(T_e)$ accounts for the finite detector resolution [15],

$$W(T_e) = \frac{1}{2}\left[{\rm Erf}\left(\frac{T_{e,2} - T_e}{\sqrt{2}\sigma_{T_e}}\right) - {\rm Erf}\left(\frac{T_{e,1} - T_e}{\sqrt{2}\sigma_{T_e}}\right)\right]. \quad (5)$$

We assume $\sigma_{T_e}/{\rm keV} = 48\sqrt{T_e/{\rm MeV}}$, as obtained by the MonteCarlo simulations of the apparatus [16].

Our reference choice for the energy window of the ν_e-e scattering experiment is $T_e \in [0.25, 0.7]$ MeV. The lower limit efficiently cuts the ^{14}C decay background, and the upper limit is safely above the Compton edge ($T_{e,\max} = 0.56$ MeV) for the electrons scattered by ^{51}Cr neutrinos. For the $\bar{\nu}_e$-e scattering we choose $T_e \in [0.25, 1]$ MeV, the upper limit now being determined by the ^{40}K contaminant [which emits γ's (B.R.=10%, $E_\gamma = 1.460$ MeV) and β's (B.R.=90%, $T_e \leq 1.32$ MeV)] in the scintillator.

For the inverse β-decay process $\bar{\nu}_e + p \to e^+ + n$, (characterized by a threshold $E_{\nu,\min} = 1.804$ MeV), the cross section is [17]

$$\sigma_e(E_\nu) = \sigma_0 \, (E_\nu - Q) \sqrt{(E_\nu - Q)^2 - m_e^2} \, , \tag{6}$$

with $\sigma_0 = 94.55 \times 10^{-45}$ cm^2/MeV^2, and $Q = 1.2933$ MeV. We actually improve Eq. (6) to account for the weak magnetism and bremsstrahlung corrections, as described in [18].

For an exposure time $t_{\rm ex}$, the expected number of events, N_0, is given by

$$N_0 = n_t \langle \sigma_e \rangle \times \int_{t_{\rm tr}}^{t_{\rm ex}+t_{\rm tr}} dt' \, I(t') \times \int_{\rm FV} \frac{d^3x}{4\pi\delta_x^2} \, , \tag{7}$$

where n_t is the volume density of targets in the fiducial volume FV, $t_{\rm tr}$ is the "transport" time elapsed from the source activation to the beginning of the source experiment, $I(t) = I_0 \exp(-t/\tau)$ is the intensity of the source ($I_0 = 5$ MCi), δ_x is the distance between the source and the generic point x in the detector volume, and

$$\langle \sigma_e \rangle = \int dE_\nu \, \lambda(E_\nu) \sigma_e(E_\nu) \, . \tag{8}$$

Given the geometry of the experiment, the integral over the volume can be performed analytically and Eq. (7) can be recast in the following, compact form:

$$N_0 = N_t \Phi_0 F(R/D) \langle \sigma_e \rangle \Gamma(t_{\rm ex}, t_{\rm tr}) \, , \tag{9}$$

where $N_t = n_t \times V$, $\Phi_0 = I_0/(4\pi D^2)$, and the function F is given by

$$F(h) = \frac{3}{2h^3} \left[h - \frac{1-h^2}{2} \ln \left(\frac{1+h}{1-h} \right) \right] \tag{10}$$

[where in our case, $F(R/D) = 1.028$] and $\Gamma(t_{\rm ex}, t_{\rm tr}) = \tau \exp(-t_{\rm tr}/\tau) \times [1 - \exp(-t_{\rm ex}/\tau)]$. We assume $t_{\rm tr} = 5$ days for both sources (Cr and Sr). For the ^{51}Cr experiment, we take $t_{\rm ex} = 60$ days, which maximizes the signal-to-noise ratio, as shown in [10]. For the ^{90}Sr experiment, the useful time limit can be determined by the condition that the statistical uncertainty of the rate reaches the size of the systematic error of the source activity (about 1%) [19]. This leads us to $t_{\rm ex} = 1/2$ years as a realistic exposure time. (A longer experiment would also interfere with the measurement of the solar ν rate, which is the main goal of BOREXINO.)

Now we discuss the background rates. For the scattering events, the background events are due both to solar neutrinos interactions and to the internal decays of radiocontaminants. The background rate R_B can be measured during the "source off" operation of the apparatus, and the number of background events is then simply given by $N_B = R_B \times t_{\rm ex}$. For Standard Solar Model expectations [20], the total background rate is expected to be $R_B = 73$ events/day for events with $T_e \in [0.25, 07]$ MeV and $R_B = 97$ events/day when $T_e \in [0.25, 1]$ MeV [10]. For the inverse β-decay events, the delayed coincidence signature allows an almost complete background rejection (apart from 10 event/year due to antineutrinos coming from nuclear reactors [21]), so we simply set $R_B \simeq 0$ in this case.

Although the background can be measured in the source off mode and subtracted from the total signal, it contributes to the uncertainties through statistical fluctuations. The total (signal+background) 1σ uncertainty of the signal is

$$\delta_{N_0} = \sqrt{N_B + N_0\,(1 + \delta_A^2 N_0)}\,, \tag{11}$$

where $\delta_A = 0.1$ is the estimated uncertainty of the source activity and errors have been added in quadrature. A deviation from the standard expectations can be evidenced at 90% C.L. if the measured rate N satisfies

$$\left|\frac{N}{N_0} - 1\right| \geq \varepsilon_{90}\,, \tag{12}$$

where $\varepsilon_{90} = 2.146 \times \delta_{N_0}/N_0$ (for the two degrees of freedom that we will consider).

Finally, in this paper we compare the BOREXINO performance with MUNU [22], a reactor experiment mounted at the Bugey laboratory, designed explicitly for studying $\bar{\nu}_e$-e scattering. MUNU has been running since August 1998. For this experiment we consider the energy window $[T_{e,1}, T_{e,2}] = [0.5, 1]$ MeV [23]. The energy resolution is $\sigma_{T_e}/\mathrm{keV} = 140\sqrt{T_e/\mathrm{MeV}}$ [24]. The energy spectrum for the $\bar{\nu}_e$ was taken from [25]. The standard expected rate is 5.3 events/day while the background is estimated in 6 events/day [23]. The uncertainty on the neutrino flux from the reactor is $\sim$5% [23]. As reference, we set $t_{\rm ex} = 1$ y.

In Tab. I we report the background, the standard expectation, the uncertainty, and the ε_{90} for the three measure (ν-e and $\bar{\nu}$-e scattering, and inverse β-decay) of interest for this paper and for the MUNU experiment.

III. PROBING FLAVOR OSCILLATIONS

Neutrino flavor oscillations [26] represent a viable solution to the so-called solar neutrino problem [27] and to the atmospheric neutrino anomaly [28]. This phenomenon can also be probed at accelerators [29–34] and reactors [35–38]. The flavor survival probability of a neutrino with energy E_ν, at a distance L from the source is

$$P(E_\nu, L) = 1 - \frac{1}{2}\sin^2 2\theta \left[1 - \cos\left(\frac{\delta m^2}{2E_\nu} L\right)\right]\,, \tag{13}$$

where θ is the mixing angle and $\delta m^2 = m_2^2 - m_1^2$ is the difference between the square of the two neutrino masses. (We have assumed only two neutrino families for simplicity).

A deficit of the measured rate in the BOREXINO source experiments might signal neutrino oscillations, i.e., the disappearance of the initial flavor ν_e into either active states (say, ν_μ) or sterile states (ν_s). We assume two-family $\nu_e \to \nu_\mu$ or $\nu_e \to \nu_s$ oscillations. In the presence of oscillations, Eq. (7) transforms in the following way:

$$N(\delta m^2, \sin^2 2\theta) = n_t \int_{t_{\rm tr}}^{t_{\rm ex}+t_{\rm tr}} dt'\, I(t') \int dE_\nu\, \lambda(E_\nu)$$

$$\times \int_{\rm FV} \frac{d^3x}{4\pi\delta_x^2} \left[\sigma_e(E_\nu) P(E_\nu, \delta_x) + \sigma_{\rm NC}(E_\nu)\,(1 - P(E_\nu, \delta_x))\right]\,. \tag{14}$$

In Eq. (14), $\sigma_{\rm NC} = \sigma_\mu$ for $\nu_e \to \nu_\mu$ and $\sigma_{\rm NC} = 0$ for $\nu_e \to \nu_s$ and inverse beta-decay. Inserting the expression for the probability (13) in Eq. (14), we obtain, through Eq. (9):

$$N(\delta m^2, \sin^2 2\theta) = N_0 \left[1 - \frac{1}{2}\sin^2 2\theta \left(1 - \rho - \gamma\left(\delta m^2\right)\right)\right] , \tag{15}$$

where N_0 is the standard expectation and

$$\rho = \frac{\int dE_\nu\, \sigma_{\rm NC}(E_\nu)\lambda(E_\nu)}{\int dE_\nu\, \sigma_e(E_\nu)\lambda(E_\nu)} = \begin{cases} 0.222 & \text{for } \nu\text{-}e \text{ scattering,} \\ 0.433 & \text{for } \bar{\nu}\text{-}e \text{ scattering,} \\ 0 & \text{for } \nu_e \to \nu_s \text{ and inverse } \beta \text{ decay,} \end{cases} \tag{16}$$

and

$$\gamma(\delta m^2) = \frac{\int dE_\nu\, \left[\sigma_e(E_\nu) - \sigma_{\rm NC}(E_\nu)\right] \lambda(E_\nu) g(R/D, \delta m^2 D/2E_\nu)}{\int dE_\nu\, \sigma_e(E_\nu)\lambda(E_\nu)} , \tag{17}$$

where the function g is given by

$$g = \frac{1}{F(R/D)} \frac{3D^2}{R^3} \int_{\rm FV} \frac{d^3x}{4\pi\delta_x^2} \cos\frac{\delta m^2 \delta_x}{2E_\nu} . \tag{18}$$

This function can be calculated analytically (see the appendix).

From Eqs. (15) and (12) we obtain a compact form for the 90% limit in the plane $(\delta m^2, \sin^2 2\theta)$:

$$\sin^2 2\theta \left(1 - \rho - \gamma\left(\delta m^2\right)\right) = 2\varepsilon_{90} , \tag{19}$$

In Fig. 2 we show the 90% C.L. contours in the plane $(\delta m^2, \sin^2 2\theta)$ for the ^{90}Sr antineutrinos in the case of ν-e scattering (short-dashed line) and inverse β-decay (dotted line), and the for ^{51}Cr neutrinos (long-dashed line), for the $\nu_e \to \nu_\mu$ [panel (a)] and $\nu_e \to \nu_s$ [panel (b)] transitions. The gray area is the combined fit (i.e., the allowed zone if no deficit were found). Superposed we show also the 90% C.L. bounds coming from negative evidence for oscillations (solid thick line) and the LSND allowed area (solid thin line).

The function $\gamma(\delta m^2)$ drops rapidly to zero for $\delta m^2 > 1$ eV^2, because of the rapid oscillation of the cosine term in Eq. (18). Consequently, for $\delta m^2 > 1$ eV^2, the testable value of $\sin^2 2\theta$ tends to the constant value $2\varepsilon_{90}/(1-\rho)$. As expected, in the case of ν-e and $\bar{\nu}$-e scattering, the sensitivity in the $\nu_e \to \nu_s$ channel is thus better, due to the absence of the ρ term. The higher statistics attainable make the ^{90}Sr source more appropriate to check lower values of $\sin^2 2\theta$ for high values of δm^2. On the other hand, the low energy of the main decay branch of the ^{51}Cr source make it more appropriate to check lower values of δm^2, although it cannot compete with the CHOOZ sensitivity.

In Fig. 2(a) and (b), the thick solid lines represent the 90% C.L. exclusion contours due to the χ^2-combination of the negative results coming from short baseline reactor experiments (Bugey [36], Krasnoyarsk [37], Gösgen [35]) and from the long baseline reactor experiment CHOOZ [38], searching for the disappearance channel ($\bar{\nu}_e \leftrightarrow \bar{\nu}_e$), together with the negative results from the accelerator experiments E776 ($\nu_\mu \leftrightarrow \nu_e$) [29], KARMEN2 ($\nu_\mu \leftrightarrow \nu_e$) [30], and CDHSW ($\nu_\mu \leftrightarrow \nu_\mu$) [31]. In the case of $\nu_e \to \nu_s$ oscillations [panel(b)] only the disappearance channel can be probed (through reactor experiments).

In the panel (a), the thin solid line defines the 90% C.L. favored region delimited by the positive signal of the LSND experiment [32] as obtained in [39]. Notice that only a very

small region of the parameter space allowed by LSND survives the comparison with negative searches.

From panel (a) of Fig. 2 we see that the zone tested by the BOREXINO source experiments, (in the hypothesis of $\nu_e \to \nu_\mu$ oscillations) is already contained in the current bounds. Therefore, if a significative difference from the standard expectation is found, it cannot be interpreted as $\nu_e \to \nu_\mu$ oscillations.

However, in the case of $\nu_e \to \nu_s$ oscillations [panel (b)] the ^{90}Sr source can improve the current bounds for $\delta m^2 > 1$ eV^2 and in the region around $(\delta m^2, \sin^2 2\theta) \sim (3 \times 10^{-1}\ \text{eV}^2, 3 \times 10^{-2})$. The higher sensitivity of BOREXINO for $\delta m^2 \to \infty$ with respect the reactor experiments is mainly due to the higher statistics and the lower background. In particular, the bound on $\sin^2 2\theta$ for $\delta m^2 \geq 3$ eV^2 can be shifted to 5×10^{-2} (4×10^{-2} if the combined fit is considered), thus improving the existing limits by about a factor 2. Moreover,since both $\bar{\nu}_e$ scattering and inverse β-decay can probe the same values of $\sin^2 2\theta$ for $\delta m^2 > 1\text{eV}^2$, cross checks are possible. If a deficit in the counting is found in both cases, this could be interpreted as a signal for $\nu_e \to \nu_s$ transition.

Finally, the ^{51}Cr experiment can strongly improve the present bounds on ν_e transitions fixed by the calibration source experiment in GALLEX [40]. In particular, in the case of $\nu_e \to \nu_\mu$ oscillations, the bound on δm^2 would be lowered by a factor 10, from $\sim 10^{-1}$ eV^2 to $\sim 10^{-2}$ eV^2. (The lower bound on $\sin^2 2\theta$ is now fixed by KARMEN to 0.052, stronger than the BOREXINO one.) In the case of $\nu_e \to \nu_s$ transition, BOREXINO would fix also the bound on $\sin^2 2\theta$ to 0.1 — two times better than GALLEX. If an oscillation signal were find in the ν_e channel but not in the $\bar{\nu}_e$ channel this would be an evidence for CP violation.

IV. IMPLICATIONS FOR NEUTRINO E.M. FORM FACTORS

Neutrinos can interact with photons through a possible magnetic dipole moment or anapole moment (also called charge radius). The effective ν-γ interaction Lagrangian is [41,42]

$$\mathcal{L}_\nu^{\text{e.m.}} = \frac{\langle r_\nu^2 \rangle}{6} \bar{\psi}_\nu \gamma_\alpha \psi_\nu \Box A^\alpha - \frac{\mu_\nu}{4m_e} \bar{\psi}_\nu \sigma_{\alpha\beta} \psi_\nu F^{\alpha\beta}\,, \tag{20}$$

where ψ_ν is the neutrino field, $\langle r_\nu^2 \rangle$ is the anapole moment and μ_ν the neutrino magnetic moment. The mere existence of a neutrino Dirac mass implies an effective neutrino magnetic moment equal to $\mu_\nu = 3.2 \times 10^{-19} \mu_B (m_\nu/\text{eV})$ [43], where $\mu_B = e/2m_e$ is the Bohr magneton. Regarding the anapole moment, the situation is controversial. Some authors assert that the effective anapole moment coming from the radiative corrections of the neutrino vertex in the Standard Model is not gauge invariant and then cannot be a physical observable [44], while in [45] it is claimed that a gauge invariant part can be extracted, yielding a value $\langle r_{\nu_e}^2 \rangle_{\text{std}} \simeq 0.4 \times 10^{-32}$ cm^2 for a top quark mass of 175 GeV. Conservatively one can say that values of this two e.m. form factors larger than quoted above would be an indication for non-standard neutrino physics.

Stringent bounds on the neutrino e.m. form factors come from astrophysical arguments. For example, if the neutrino anapole moment exceeds $\sim 7 \times 10^{-32}$ cm^2, escaping neutrinos would overcool stars and hence should modify the color-magnitude diagram of globular

clusters [42]. Moreover, the energy loss in red giants in globular clusters via the plasmon decay $\gamma^* \to \nu_R \bar{\nu}_R$ mediated by neutrino magnetic moment would be too large [46] unless $\mu_\nu \leq 2 \times 10^{-12} \mu_B$. A rather stringent limit comes also from the SN1987A, $\mu_\nu \leq 5 \times 10^{-13} \mu_B$ [47].

However, the only direct experimental constraint on the ν_e magnetic moment ($\mu_{\nu_e} < 1.8 \times 10^{-10} \mu_B$), comes from reactor experiments sensitive to $\bar{\nu}_e$-e^- elastic scattering [48]. As regard the electron neutrino anapole moment $\langle r^2_{\nu_e} \rangle$, the more stringent limit comes from the LAMPF Collaboration which quotes $-7.6 \leq \langle r^2_{\nu_e} \rangle / 10^{-32} \mathrm{cm}^2 \leq 10.5$ [49,42]. Improved bounds are expected from MUNU [22]. In the following, we will also discuss this experiment in comparison with BOREXINO.

The possibility to search for a neutrino magnetic moment using an external neutrino source was addressed by the BOREXINO Collaboration in 1991 [2] and then studied in [9] and [10]. In this section we study ν-e scattering process in the general case, i.e., with non-zero magnetic and anapole moments.

From the Lagrangian in Eq. (20), the ν_e-e differential cross section is obtained [41,42]:

$$\frac{d\sigma(E_\nu, T_e)}{dT_e} = \frac{d\sigma^{\mathrm{std}}(E_\nu, T_e)}{dT_e} + \frac{\pi \alpha^2_{\mathrm{e.m.}} \mu^2_\nu}{m^2_e} \left(\frac{1}{T_e} - \frac{1}{E_\nu} \right)$$

$$+ \langle r^2_\nu \rangle \frac{\sqrt{2} G_F m_e}{3} \left[(C_V + C_A) + (C_V - C_A) \left(1 - \frac{T_e}{E_\nu} \right)^2 - C_V \frac{m_e T_e}{E^2_\nu} \right]$$

$$+ \langle r^2_\nu \rangle^2 \frac{\pi \alpha^2_{\mathrm{e.m.}} m_e}{9} \left[1 + \left(1 - \frac{T_e}{E_\nu} \right)^2 - \frac{m_e T_e}{E^2_\nu} \right] . \qquad (21)$$

The number of observed events as function of the e.m. form factors is given by:

$$N(\mu_\nu, \langle r^2_\nu \rangle) = N_0 \left[1 + \frac{\langle \sigma^M \rangle}{\langle \sigma^{\mathrm{std}} \rangle} \mu^2_\nu + \frac{\langle \sigma^{R1} \rangle}{\langle \sigma^{\mathrm{std}} \rangle} \langle r^2_\nu \rangle + \frac{\langle \sigma^{R2} \rangle}{\langle \sigma^{\mathrm{std}} \rangle} \langle r^2_\nu \rangle^2 \right] , \qquad (22)$$

where N_0 is the standard expectation, and $\langle \sigma^M \rangle$, $\langle \sigma^{R1} \rangle$, and $\langle \sigma^{R2} \rangle$ are the partial cross section in Eq. (21) integrated on the electron recoil energy [including the corrections due to the finite resolution of the detector, according to Eq. (4)] and folded with the source spectrum. From Eqs. (22) and (12) we obtain the equation for 90% sensitivity bound in the plane $(\langle r^2_\nu \rangle, \mu_\nu)$ for a null result:

$$\mu_\nu = \left[\pm \eta_0 - \eta_1 \langle r^2_\nu \rangle - \eta_2 \langle r^2_\nu \rangle^2 \right]^{1/2} , \qquad (23)$$

where $\eta_0 = \langle \sigma^{\mathrm{std}} \rangle \varepsilon_{90} / \langle \sigma^M \rangle$ and $\eta_{1,2} = \langle \sigma^{R1,2} \rangle / \langle \sigma^M \rangle$. In Tab. II we report our calculation of the coefficients η_0, η_1, and η_2 for the cases of ^{51}Cr and ^{90}Sr source experiments, and for the MUNU experiment, where μ_ν is measured in units of $10^{-10} \mu_B$ and $\langle r^2_\nu \rangle$ in units of 10^{-32} cm^2.

In Fig. 3 we show the 90% C.L. contours for ^{51}Cr neutrinos (dashed lines) and ^{90}Sr antineutrinos (dotted lines). The shaded line is the limit on $\langle r^2_\nu \rangle$ set by LAMPF [49]. If no difference with the standard expectation were found, combining this limit with the BOREXINO measurement one can put an upper limit on μ_ν equal to $0.8 \times 10^{-10} \mu_B$ (90% C.L. for 2 d.o.f.) for neutrinos and $0.6 \times 10^{-10} \mu_B$ for antineutrinos. Moreover, one can put

an upper limit on $\langle r_\nu^2 \rangle$ equal to $\simeq 2 \times 10^{-32}$ cm^2 for neutrinos and $\simeq 0.5 \times 10^{-32}$ cm^2 for antineutrinos, close to the value in [45]. Moreover, assuming that the magnetic and anapole moment are equal for neutrinos and antineutrinos, it is possible to perform a combined fit (gray area in Fig. 3). In this case, one obtains a more stringent bound on the parameters: $-5.5 \leq \langle r_\nu^2 \rangle / 10^{-32}$ cm$^2 \leq 0.5$ and $\mu_\nu \leq 0.55 \times 10^{-10} \mu_B$.

In Fig. 3 we show for comparison the zone explorable by the MUNU experiment after one year of operation (solid line). For $\langle r_\nu^2 \rangle$ unconstrained, MUNU can put a limit $\mu_\nu \leq 0.85 \times 10^{-10} \mu_B$. For $\langle r_\nu^2 \rangle = 0$, we obtain a limit $\mu_\nu \leq 0.42 \times 10^{-10} \mu_B$ (90% C.L. for 1 d.o.f.), [2] in relatively good agreement with the MUNU collaboration analysis [23].

From Fig. 3 we see that both the ^{51}Cr and the ^{90}Sr limits are more stringent then those expected in MUNU as a result of higher statistics, of the smaller flux uncertainties, and of the lower energy threshold of BOREXINO. In particular, the ^{90}Sr $\bar{\nu}$ experiment is the most sensitive. For $\langle r_\nu^2 \rangle = 0$, the ^{90}Sr limit on μ_ν is $0.16 \times 10^{-10} \mu_B$ (90% C.L. for 1 d.o.f.), about three times better than MUNU. This limit depends weakly on assumptions about the source activity and exposure time. For example, with 2.5 MCi activity and 3 months of exposure, this limit is raised to $0.21 \times 10^{-10} \mu_B$ — about a factor two better than MUNU. In fact, for $\langle r_\nu^2 \rangle = 0$, the limit value of μ_ν depends on the square root of ε_{90} [see Eq. (23)]. This make this experiment very appropriate for magnetic moment searches.

V. IMPLICATIONS FOR VECTOR AND AXIAL COUPLINGS

The low energy ν-e neutral current interaction is usually parameterized by the following effective four-fermion Hamiltonian:

$$\mathcal{H}_{\rm int}^{\nu e} = -\frac{G_F}{\sqrt{2}} \left[\bar{\psi}_\nu \gamma^\alpha \left(1 - \gamma^5\right) \psi_\nu \right] \left[\bar{\psi}_e \gamma_\alpha \left(g_V^{\nu e} - g_A^{\nu e} \gamma^5 \right) \psi_e \right] , \tag{24}$$

where ψ_ν and ψ_e are the neutrino and electron fields and $g_{V,A}^{\nu e}$ are the vector and axial coupling of the neutrino current to the electron current. When also charge current interactions are involved, as in the case of ν_e-e scattering, $g_{V,A}^{\nu e} \to g_{V,A}^{\nu e} + 1$.

The Standard Model of electroweak interactions states that $g_V^{\nu e} = 2 \sin^2 \theta_W - \frac{1}{2} = (-0.038)$ and $g_A^{\nu e} = -1/2$, apart from small radiative corrections. Moreover, in the Standard Model $g_{V,A}^{\nu e} = g_{V,A}^{\nu} \cdot g_{V,A}^{e}$, where $g_{V,A}^{\nu}$ ($g_{V,A}^{e}$) are the couplings of the neutrinos (electrons) to the Z boson. The values of $g_{V,A}^{\nu}$ are inferred from the "invisible" decay width of the Z boson [50,7]. Although this gives the value of $g_{V,A}^{\nu e,\rm std}$ with great precision, it does not account for possible non-standard process occurring in the ν-e scattering. (for example, exchange of non-standard neutral gauge boson, as proposed in [11]). For this reason, a direct measure of the $g_{V,A}^{\nu e}$ couplings is interesting.

At present, the most precise *direct* determinations of $g_{V,A}^{\nu e}$, come from the CHARM II experiment using ν_μ-e scattering [51]: $g_V^{\nu e} = -0.035 \pm 0.017$ and $g_A^{\nu e} = -0.503 \pm 0.017$ at 1σ, in agreement with Standard Model. In this section, we investigate the possibility to

[2] When only 1 d.o.f. is concerned, ε_{90} have to be reduced by a factor 0.767.

probe $g_{V,A}^{\nu e}$ using the BOREXINO calibration experiments. From Eq. (24), one obtains the differential cross section for ν_e-e scattering [14] in the form of Eq. (3) with $C_{V,A} = g_{V,A}^{\nu e} + 1$ where $g_{V,A}^{\nu e}$ are now independent variables. Expanding Eq. (3) in term of $g_V^{\nu e}$ and $g_A^{\nu e}$, and following the same procedure of the previous section we obtain $N(g_V^{\nu e}, g_A^{\nu e}) = N_0 f(g_V^{\nu e}, g_A^{\nu e})$ where N_0 is the standard expectation and

$$f(g_V^{\nu e}, g_A^{\nu e}) = \xi_V (g_V^{\nu e} + 1)^2 + \xi_A (g_A^{\nu e} + 1)^2 + \xi_{VA} (g_V^{\nu e} + 1)(g_A^{\nu e} + 1)\,. \tag{25}$$

Here $\xi_V = \langle \sigma(C_V = 1, C_A = 0) \rangle / \langle \sigma^{\rm std} \rangle$, $\xi_A = \langle \sigma(C_V = 0, C_A = 1) \rangle / \langle \sigma^{\rm std} \rangle$, and $\xi_{VA} = \langle \sigma(C_V = 1, C_A = 1) \rangle / \langle \sigma^{\rm std} \rangle - \xi_V - \xi_A$ [ξ_{VA} have opposite sign for $\bar{\nu}$]. In Tab. III we show the value of the coefficients ξ_V, ξ_A, and ξ_{VA} for the cases of ^{51}Cr and ^{90}Sr source experiments, and for the MUNU experiment.

From Eq. (12) we then obtain the 90% limit in the plane $(g_V^{\nu e}, g_A^{\nu e})$ for a null result:

$$f(g_V^{\nu e}, g_A^{\nu e}) = 1 \pm \varepsilon_{90}\,. \tag{26}$$

This limit is shown in Fig. 4 for the ^{51}Cr experiment (dashed line), the ^{90}Sr experiment (dotted line), and their combination (gray area). Also shown are the CHARM II results and the zone explorable by MUNU (solid line). In BOREXINO, a significative improvement in the measure of $g_V^{\nu e}$ appears possible, whilst the constraints on $g_A^{\nu e}$ are similar to CHARM II. In particular, we obtain $-0.056 \leq g_V^{\nu e} \leq -0.020$ ($0.222 \leq \sin^2\theta_W \leq 0.240$) and $-0.54 \leq g_A^{\nu e} \leq -0.46$ at the 90% C.L. (2 d.o.f.). The $\sin^2\theta_W$ is thus measured with a precision of $\sim 4\%$ — a factor two better than CHARM II. Fixing $g_A^{\nu e}$ to $-1/2$, we obtain a more stringent constraint on the Weinberg angle: $0.226 \leq \sin^2\theta_W \leq 0.236$ (90% C.L. for 1 d.o.f.), corresponding to a precision of $\sim 2.5\%$.

From Fig. 4 we can see that the BOREXINO constraints are more stringent than MUNU as a result of higher statistics attainable and of the combination of ν and $\bar{\nu}$ signal.

Finally, we stress that a comparison of scattering experiment of the kind ν_e-e (BOREXINO) and ν_μ-e (CHARM II) is a useful check of the universality of weak interactions at low energies.

VI. CONCLUSIONS

In this paper we have explored the possibility to search for non-standard neutrino properties with the BOREXINO Cr and Sr source experiments. In particular, we have considered a) Neutrino oscillations; b) Non-zero electron neutrino e.m. form factors μ_ν and $\langle r_\nu^2 \rangle$; c) Non-standard ν-e vector and axial couplings. In case a) we find that, in the channel $\nu_e \to \nu_s$, BOREXINO can extend the oscillation parameter limits for $\delta m^2 \geq 3$ eV^2 and $0.04 \leq \sin^2 2\theta \leq 0.1$. In case b) BOREXINO can reach a sensitivity to the magnetic moment equal to $0.8 \times 10^{-10} \mu_B$ for neutrinos and $0.6 \times 10^{-10} \mu_B$ for antineutrinos. In additions, assuming that the e.m. form factors are equal for ν and $\bar{\nu}$, this limit can be improved ($\mu_\nu \leq 0.5 \times 10^{-10} \mu_B$) and a limit of $-5.5 \leq \langle r_\nu^2 \rangle / 10^{-32} {\rm cm}^2 \leq 0.5$ can be put on the anapole moment — the strongest limit at present. In the hypothesis that $\langle r_\nu^2 \rangle = 0$, the ^{90}Sr experiment alone can put a limit $\mu_\nu \leq 0.16 \times 10^{-10} \mu_B$, improving the MUNU sensitivity by a factor three. In case c), BOREXINO can reduce the present uncertainty on the *direct* measure of

the $g_V^{\nu e}$ coupling by a factor 2, and can check for the universality of the ν-e interactions at low energies. Fixing $g_A^{\nu e}$ to 1/2, the Weinberg angle $\sin^2\theta_W$ can be measured with an accuracy of $\pm 2.5\%$.

VII. ACKNOWLEDGMENTS

We thank E. Lisi for useful suggestions and for careful reading of the manuscript, and J.N. Bahcall, V.V. Sinev, and J.W.F. Valle for suggestions. The work of A.I. and G.S. was supported in part by Ministero della Ricerca Scientifica (Dottorato di Ricerca) and in part by INFN. The work of D.M. was supported by INFN.

APPENDIX: CALCULATION OF THE FUNCTION g

In this Appendix we give the analytical expression for the function g of Eq. (18). In polar coordinates (choosing the z axis as the FV center-to-source direction), Eq. (18) reads

$$g = \frac{3}{2}\frac{1}{F(R/D)}\frac{D^2}{R^3}\int_0^R r^2 dr \int_0^\pi \sin\varphi d\varphi \,\frac{1}{\delta_x^2}\cos\frac{\delta m^2}{2E_\nu}\delta_x \,, \tag{A1}$$

with $\delta_x^2 = r^2 + D^2 - 2rD\cos\varphi$. With the substitutions $x = r/D$ and $y = \beta\delta_x/D$ (with $\beta = \delta m^2 D/2E_\nu$) one has

$$\begin{aligned} g &= \frac{3}{2}\frac{1}{h^3 F(h)}\int_0^h x dx \int_{\beta(1-x)}^{\beta(1+x)} dy\,\frac{\cos y}{y} \\ &= \frac{3}{2}\frac{1}{h^3 F(h)}\int_0^h x dx\,\left[\mathrm{Ci}\left(\beta(1-x)\right) - \mathrm{Ci}\left(\beta(1+x)\right)\right] \,, \end{aligned} \tag{A2}$$

where $h = R/D$ and the function $\mathrm{Ci}(z)$ is the integral cosine:

$$\mathrm{Ci}(z) = -\int_z^\infty dq\,\frac{\cos q}{q} \,. \tag{A3}$$

The integral in Eq. (A2) can be easily evaluated with the help of the following expressions:

$$\begin{aligned} \int dz\,\mathrm{Ci}(z) &= z\mathrm{Ci}(z) - \sin z \,, \\ \int dz\, z\mathrm{Ci}(z) &= \frac{z^2}{2}\mathrm{Ci}(z) - \frac{1}{2}(\cos z + z\sin z) \,. \end{aligned} \tag{A4}$$

The final result can be cast in the following form:

$$g(h,\beta) = \frac{3}{4}\frac{G\left((1+h)\beta,\beta\right) - G\left((1-h)\beta,\beta\right)}{h^3\beta^2 F(h)} \,, \tag{A5}$$

where

$$G(z,\beta) = \left[z\mathrm{Ci}(z) - \sin z\right](z - 2\beta) - \cos z \,. \tag{A6}$$

REFERENCES

[1] BOREXINO Collaboration, G. Alimonti *et al.*, *A real time detector for low energy solar neutrinos*, proposal to the National Science Foundation, edited by F.P. Calaprice *et al.* (Princeton, New Jersey, 1996).

[2] BOREXINO Collaboration, C. Arpesella *et al.*, INFN BOREXINO proposal, Vols. 1 and 2, edited by G. Bellini, R. Raghavan, *et al.* (University of Milano, 1992); J. Bezinger, F.P. Calaprice *et al.*, proposal for BOREXINO to National Science Foundation (Princeton, 1992); J. Bezinger *et al.*, *A Proposal for Participation in the BOREXINO Solar Neutrino Experiment*, Princeton University Report, 1996 (unpublished).

[3] Current information on the status of BOREXINO experiment can be retrieved from the following URL: http://almime.mi.infn.it∼.

[4] R.S. Raghavan, Science **267**, 45 (1995).

[5] J.C. Maneira, in *Proceedings of the II meeting on New Worlds in Astroparticle Physics, Faro, 1998*, to appear.

[6] E.J. Konopinski, *The theory of beta radioactivity* (Clarendon, Oxford 1966).

[7] Particle Data Group, C. Caso *et al.*, Europ. Phys. Jour. C **3**, 1 (1998).

[8] BOREXINO Collaboration, G. Alimonti *et al.*, *Proposal for a Real Time Detector for Low energy Solar neutrinos*, edited by G. Bellini *et al.* (Milano, 1991).

[9] N. Ferrari, G. Fiorentini, and B. Ricci, Phys. Lett. B **387**, 427 (1996).

[10] A. Ianni and D. Montanino, INFN-AE-98-12, to appear in Astropart. Phys.

[11] O.G. Miranda, V. Semikoz, and J.W.F. Valle, Phys. Rev. D **58** 013007 (1998); also in *Proceedings of the International symposium on lepton and baryon number violation, Trento, 1998*, to appear, hep-ph/9808395.

[12] L.A. Mikaélyan, V.V. Sinev, and S.A. Fayans, JETP Lett. **67**, 453 (1998).

[13] I.R. Barbanov *et al.*, Astropart. Phys. **8**, 67 (1997).

[14] G. t'Hooft, Phys. Lett. B **37**, 195 (1971).

[15] B. Faïd, G.L. Fogli, E. Lisi, and D. Montanino, Astropart. Phys. **10**, 93 (1999).

[16] M. Giammarchi (private communication).

[17] H. Yamaguchi, Progr. Theor. Phys. **23**, 1117 (1960).

[18] P. Vogel, Phys. Rev. D **29**, 1918 (1984); S.A. Fayans, Yad. Fiz. **42**, 929 (1985) [Sov. J. Nucl. Phys. **42**, 590 (1985)].

[19] M. Cribier *et al.*, Nucl. Instrum. Meth. A **378**, 233 (1996); B.R. Bergelson, A.V. Davydov, Yu.N. Isaev, and V.N. Kornoukhov, Phys. Atom. Nucl. **61**, 1245 (1998).

[20] J.N. Bahcall and M.H. Pinsonneault, Rev. Mod. Phys. **67**, 781 (1995).

[21] S. Schoenert, in *Proceedings of TAUP'97, V International Workshop on Topics in Astroparticle and Underground Physics, Gran Sasso Laboratory, 1997*, edited by A. Bottino, A. Di Credico, and P. Monacelli, Nucl. Phys. B Proc. Suppl. **70**, 195 (1999).

[22] C. Broggini *et al.*, Nucl. Phys. B **35**, 441 (1994).

[23] C. Broggini in *TAUP'97* [21], p. 188.

[24] G. Jonkmans, in *Neutrino'98, Proceedings of the XVIII International Conference on Neutrino Physics and Astrophysics, Takayama, 1998*, to appear.

[25] A.M. Bakalyarov, V.I. Kopeikin, and L.A. Mikaelian, Phys. Atom. Nucl. **59**, 1771 (1996); V.I. Kopeikin, L.A. Mikaelyan, and V.V. Sinev, Phys. Atom. Nucl. **60**, 172 (1997).

[26] B. Pontecorvo, Zh. Eksp. Teor. Fiz. **53**, 1717 (1967) [Sov. Phys. JETP **26**, 984 (1968)]; V. Gribov and B. Pontecorvo, Phys. Lett. B **28**, 493 (1969).
[27] J.N. Bahcall, *Neutrino Astrophysics* (Cambridge University Press, Cambridge, 1989).
[28] M. Honda, T. Kajita, K. Kasahara, and S. Midorikawa, Phys. Rev. D **52**, 4985 (1995); V. Agrawal, T.K. Gaisser, P. Lipari, and T. Stanev, Phys. Rev. D **53** 1314 (1996).
[29] E776 Collaboration, L. Borodovsky *et al.*, Phys. Rev. Lett. **68**, 274 (1992).
[30] KARMEN Collaboration, K. Eitel *et al.*, report hep-ex/9809007, in *Neutrino'98* [24]; B. Zeitnitz *et al.*, Prog. Part. Nucl. Phys. **40**, 169 (1998).
[31] CDHSW Collaboration, F. Dydak *et al.*, Phys. Lett. B **134**, 281 (1984).
[32] LSND Collaboration, C. Athanassopoulos *et al.*, Phys. Rev. C **54**, 2685 (1996).
[33] E531 Collaboration, N. Ushida *et al.*, Phys. Rev. Lett. **57**, 2897 (1986).
[34] KARMEN Collaboration, B. Armbruster *et al.*, Phys. Rev. C **57**, 3414 (1998).
[35] G. Zacek *et al.*, Phys. Rev. D **34**, 2621 (1986).
[36] B. Achkar *et al.*, Nucl. Phys. B **434**, 503 (1995).
[37] G.S. Vidyakin *et al.*, Pis'ma Zh. Eksp. Teor. Fiz. **59**, 364 (1994) [JETP Lett. **59**, 390 (1994)].
[38] CHOOZ Collaboration, M. Apollonio *et al.*, Phys. Lett. B **420**, 397 (1998).
[39] G.L. Fogli, E. Lisi, G. Scioscia, Phys. Rev. D **56**, 3081 (1997).
[40] GALLEX collaboration, P. Anselmann *et al.*, Phys. Lett. B **342**, 440 (1995); J.N. Bahcall, P.I. Krastev, and E. Lisi, Phys. Lett. B **348**, 121 (1995).
[41] P. Vogel and J. Engel, Phys. Rev. D **39**, 3378 (1989).
[42] P. Salati, Astropart. Phys. **2**, 269 (1994).
[43] B.W. Lee and R.E. Schrock, Phys. Rev. D **16**, 1444 (1977); W. Marciano and A.I. Sanda, Phys. Lett. B **67**, 303 (1977); K. Fujikawa and R.E. Schrock, Phys. Rev. Lett. **45**, 963 (1980).
[44] W.A. Bardeen, R. Gastmans, and B. Lautrup, Nucl. Phys. B **46**, 319 (1972); N.M. Monyonko and J.H. Reid, Prog. Theor. Phys. **73**, 734 (1985); J.L. Lucio, A. Rosado, and A. Zepeda, Phys. Rev. D **39**, 1091 (1985); M.J. Musolf and B.R. Holstein, Phys. Rev. D **43**, 2965 (1991).
[45] G. Degrassi, W.J. Marciano, and A. Sirlin, Phys. Rev. D **39**, 287 (1989).
[46] G. Raffelt, Astrophys. J. **365**, 559 (1990).
[47] J.M. Lattimer and J. Coopersteim, Phys. Rev. Lett. **61**, 23 (1988); A. Barbieri and R.N. Mohapatra, Phys. Rev. Lett. **61**, 27 (1988); D. Nötzold, Phys. Rev. D **38**, 1658 (1988); A. Goyal, S. Dutta, and S.R. Choudhury, Phys. Lett. B **49**, 312 (1995).
[48] A.V. Derbin, Phys. Atom. Nucl. **57**, 222 (1994).
[49] LAMPF Collaboration, R.C. Allen *et al.*, Phys. Rev. D **47**, 11 (1993).
[50] The LEP Collaborations, ALEPH, DELPHI, L3, and OPAL, Phys. Lett. B **276**, 247 (1992).
[51] CHARM II Collaboration, P. Vilain *et al.*, Phys. Lett. B **335**, 246 (1994).

TABLES

TABLE I. Time of exposure ($t_{\rm ex}$), expected background events (N_B), standard signal events (N_0), 1σ uncertainty of N_0 (δ_{N_0}), and 90% C.L. (2 d.o.f.) relative accuracy for the ν-e scattering, $\bar{\nu}$-e scattering, inverse β-decay, and MUNU experiments.

experiment	reaction	$t_{\rm ex}$ (days)	N_B	$N_0 \pm \delta_{N_0}$	ε_{90}
^{51}Cr	ν_e-e scat.	60	4380	4006 ± 100	5.4×10^{-2}
^{90}Sr	$\bar{\nu}_e$-e scat.	180	17460	25971 ± 333	2.8×10^{-2}
^{90}Sr	inv. β-decay	180	~ 5	13278 ± 176	2.8×10^{-2}
MUNU	$\bar{\nu}_e$-e scat.	365	2190	1935 ± 116	12.9×10^{-2}

TABLE II. Coefficients η of Eq. (23) for the BOREXINO ^{51}Cr and ^{90}Sr source experiments, and for MUNU. See the text for details.

source	η_0	η_1	η_2
^{51}Cr	0.139	7.7×10^{-2}	6.4×10^{-4}
^{90}Sr	0.033	5.3×10^{-2}	9.1×10^{-4}
MUNU	0.234	8.3×10^{-2}	1.4×10^{-3}

TABLE III. Coefficients ξ of Eq. (25) for the BOREXINO ^{51}Cr and ^{90}Sr source experiments, and for MUNU. See the text for details.

source	ξ_V	ξ_A	ξ_{VA}
^{51}Cr	0.441	0.825	0.799
^{90}Sr	1.392	1.849	−1.558
MUNU	1.359	1.695	−1.422

FIGURES

FIG. 1. Spectrum of the ^{90}Sr antineutrino source.

FIG. 2. Prospective 90% C.L. sensitivity contours in the oscillation parameters plane for the BOREXINO source experiments in the case of $\nu_e \to \nu_\mu$ and $\nu_e \to \nu_s$ transitions [panel (a) and (b), respectively]. Short-dashed line: ν-e scattering of the ^{90}Sr antineutrinos; long-dashed line: ν-e scattering of the ^{51}Cr neutrinos; dotted line: inverse β-decay; gray area: combined Sr+Cr experiments. The 90% C.L. limits coming from negative evidences of oscillations (solid thick line) and the LSND allowed area (thin solid line) are also shown.

FIG. 3. Prospective 90% C.L. sensitivity contours in the neutrino e.m. form factors plane for the BOREXINO source experiments. Dashed line: ^{51}Cr neutrinos; dotted line: ^{90}Sr antineutrinos; gray area: combined Sr+Cr experiments. The 90% C.L. LAMPF limit on $\langle r^2_{\nu_e} \rangle$ (shaded line) and the expected 90% C.L. MUNU limit (solid line) are also shown.

FIG. 4. Prospective 90% C.L. sensitivity contours in the ν-e vector and axial coupling plane for the BOREXINO source experiments. Dashed line: ^{51}Cr neutrinos; dotted line: ^{90}Sr antineutrinos; gray area: combined Sr+Cr experiments. The 90% C.L. data from CHARM II data and the expected 90% C.L. MUNU limit (solid line) are also shown.

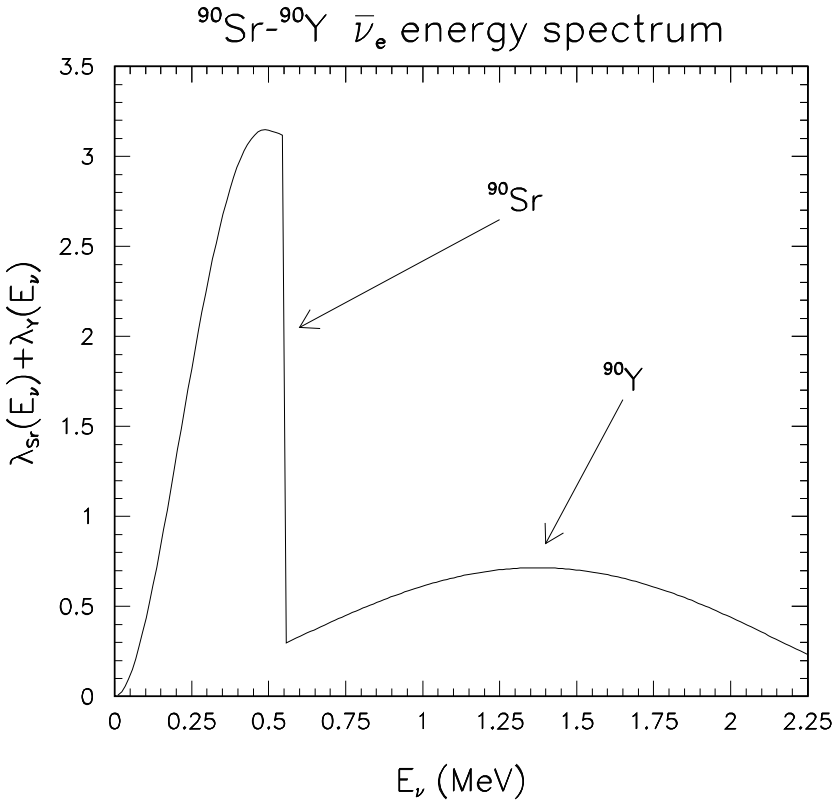

Fig. 1. Spectrum of the ^{90}Sr antineutrino source.

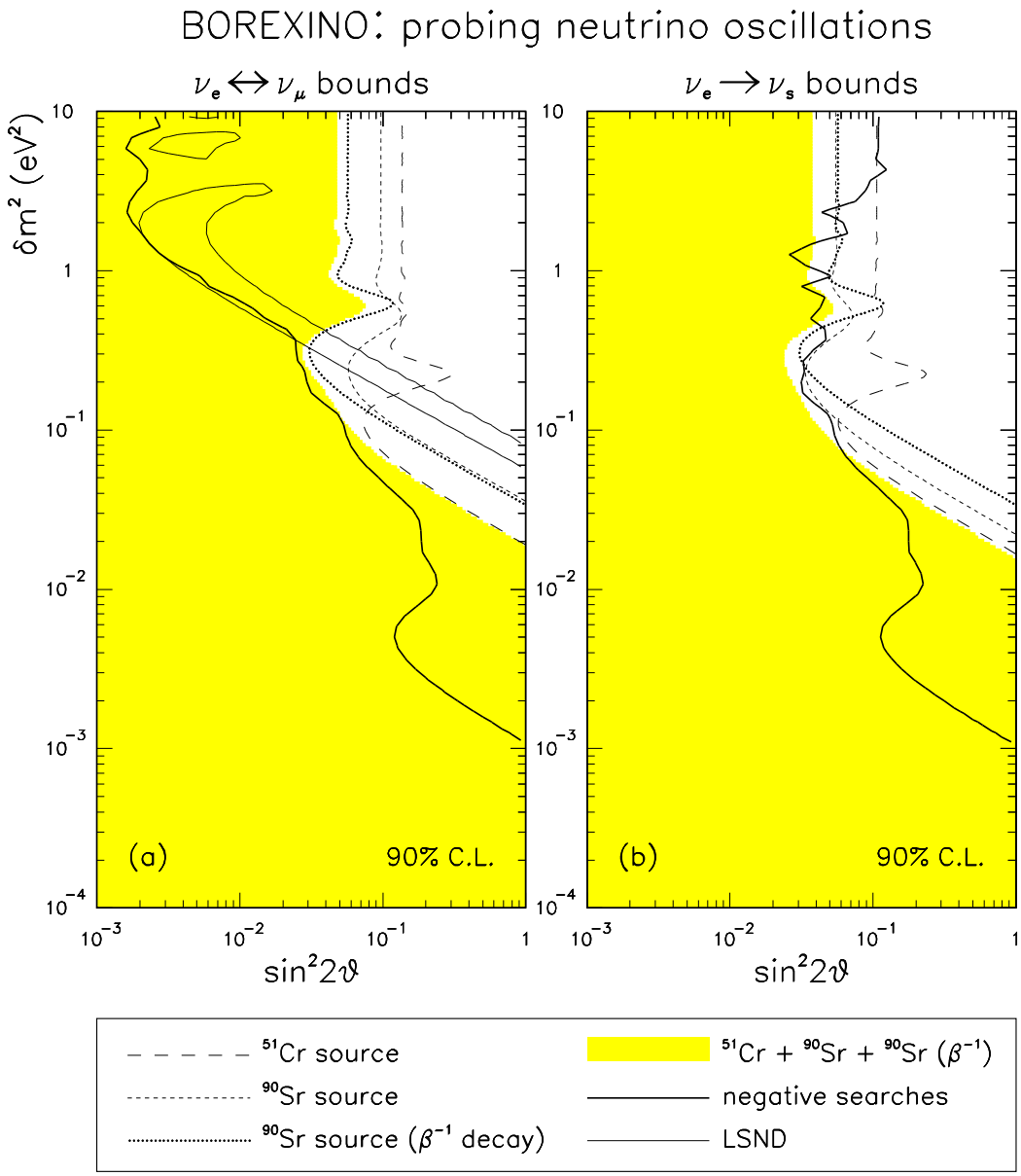

FIG. 2. Prospective 90% C.L. sensitivity contours in the oscillation parameters plane for the BOREXINO source experiments in the case of $\nu_e \rightarrow \nu_\mu$ and $\nu_e \rightarrow \nu_s$ transitions [panel (a) and (b), respectively]. Short-dashed line: ν-e scattering of the ^{90}Sr antineutrinos; long-dashed line: ν-e scattering of the ^{51}Cr neutrinos; dotted line: inverse β-decay; gray area: combined Sr+Cr experiments. The 90% C.L. limits coming from negative evidences of oscillations (solid thick line) and the LSND allowed area (thin solid line) are also shown.

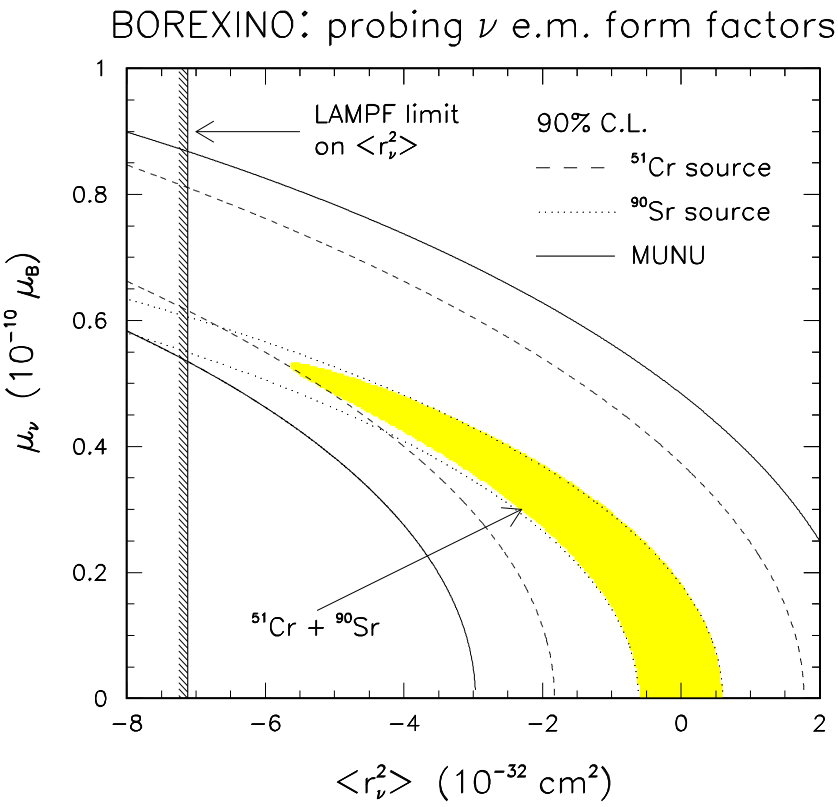

FIG. 3. Prospective 90% C.L. sensitivity contours in the neutrino e.m. form factors plane for the BOREXINO source experiments. Dashed line: ^{51}Cr neutrinos; dotted line: ^{90}Sr antineutrinos; gray area: combined Sr+Cr experiments. The 90% C.L. LAMPF limit on $\langle r^2_{\nu_e} \rangle$ (shaded line) and the expected 90% C.L. MUNU limit (solid line) are also shown.

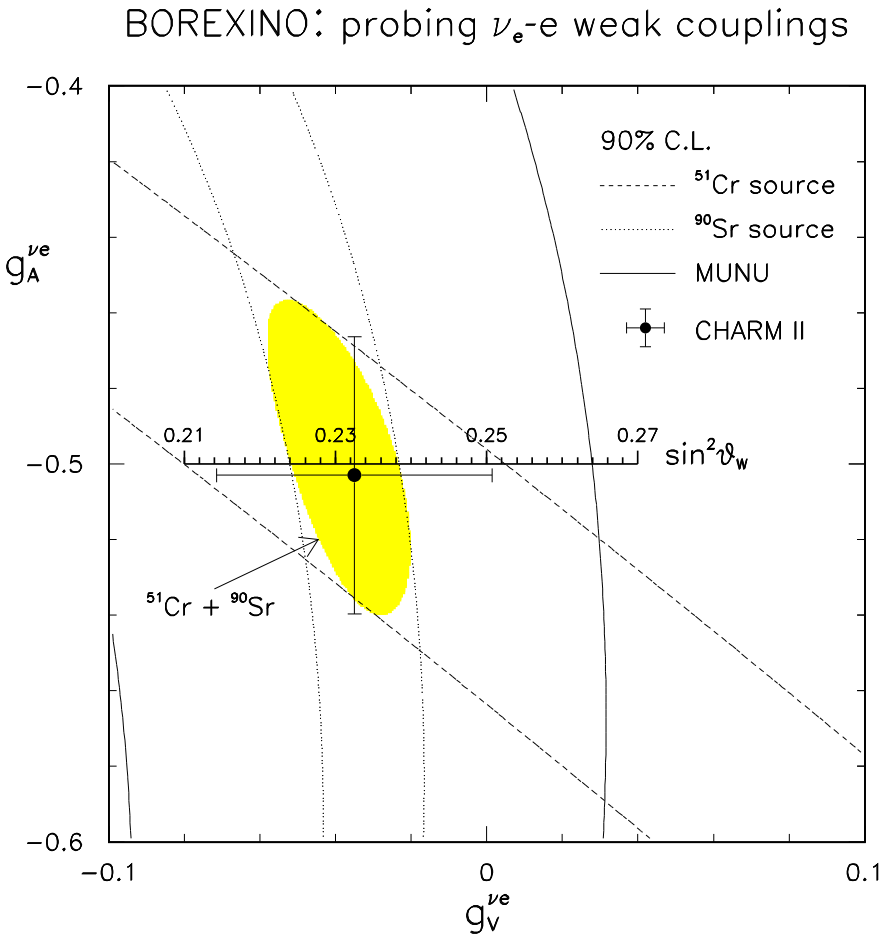

FIG. 4. Prospective 90% C.L. sensitivity contours in the ν-e vector and axial coupling plane for the BOREXINO source experiments. Dashed line: ^{51}Cr neutrinos; dotted line: ^{90}Sr antineutrinos; gray area: combined Sr+Cr experiments. The 90% C.L. data from CHARM II data and the expected 90% C.L. MUNU limit (solid line) are also shown.